British Journal of Pharmacology

DOI:10.1111/bph.12188
www.brjpharmacol.org

RESEARCH PAPER

Inhibition of iPLA$_2$β and of stretch-activated channels by doxorubicin alters dystrophic muscle function

H M Ismail[1,2], O M Dorchies[1,3], R Perozzo[2], M K Strosova[1], L Scapozza[2] and U T Ruegg[1]

[1]*Pharmacology, Geneva–Lausanne School of Pharmaceutical Sciences, University of Geneva and University of Lausanne, Geneva, Switzerland,* [2]*Pharmaceutical Biochemistry, Geneva–Lausanne School of Pharmaceutical Sciences, University of Geneva and University of Lausanne, Geneva, Switzerland, and* [3]*Department of Cell Biology, University of Geneva, Geneva, Switzerland*

Correspondence
Urs T Ruegg, Pharmacology, Geneva–Lausanne School of Pharmaceutical Sciences, University of Geneva and University of Lausanne, 30 Quai Ernest-Ansermet, 1211, Geneva 4, Switzerland. E-mail: urs.ruegg@unige.ch

Keywords
dystrophin; mdx; doxorubicin; muscle; calcium; PLA$_2$; stretch-activated channels; store-operated channels; aequorin; reactive oxygen species

Received
12 September 2012
Revised
28 February 2013
Accepted
15 March 2013

BACKGROUND AND PURPOSE

Chronic elevation in intracellular Ca^{2+} concentration participates in death of skeletal muscle from mdx mice, a model for Duchenne muscular dystrophy (DMD). Candidate pathways mediating this Ca^{2+} overload involve store-operated channels (SOCs) and stretch-activated channels (SACs), which are modulated by the Ca^{2+}-independent form of PL A_2 (iPLA$_2$). We investigated the effect of doxorubicin (Dox), a chemotherapeutic agent reported to inhibit iPLA$_2$ in other systems, on the activity of this enzyme and on the consequences on Ca^{2+} handling and muscle function in mdx mice.

EXPERIMENTAL APPROACH

Effects of Dox on iPLA$_2$ activity, reactive oxygen species production and on Ca^{2+} influx were investigated in C2C12 and mdx myotubes. The mechanism of Dox-mediated iPLA$_2$ inhibition was evaluated using purified 6x histidine-tagged enzyme. Aequorin technology was used to assess Ca^{2+} concentrations underneath the plasma membrane. Isolated muscles were exposed to fatigue protocols and eccentric contractions to evaluate the effects of Dox on muscle function.

KEY RESULTS

Dox at 1–30 μM inhibited iPLA$_2$ activity in cells and in the purified enzyme. Dox also inhibited SAC- but not SOC-mediated Ca^{2+} influx in myotubes. Stimulated elevations of Ca^{2+} concentrations below the plasmalemma were also blocked. Exposure of excised muscle to Dox was not deleterious to force production and promoted recovery from eccentric contractions.

CONCLUSIONS AND IMPLICATIONS

Dox showed efficacy against targets known to play a role in the pathology of DMD, namely iPLA$_2$ and SAC. The potent SAC inhibitory effect of Dox is a novel finding that can explain partly the cardiomyopathy seen in chronic anthracycline treatment.

Abbreviations

$AACOCF_3$, arachidonyl trifluoromethyl ketone; BEL, bromoenol lactone; DMD, Duchenne muscular dystrophy; DMEM, Dulbecco's modified minimal essential medium; Dox, doxorubicin; EDL, extensor digitorum longus muscle; iPLA$_2$, Ca^{2+} independent phospholipase A_2; L_0, optimum length; MAFP, methyl arachidonyl fluorophosphonate; NOX, NADPH oxidases; PSS, physiological salt solution; ROS, reactive oxygen species; SAC, stretch-activated channels; SOC, store-operated channels; SOL, soleus muscle

Introduction

Duchenne muscular dystrophy (DMD) represents the most frequent muscular dystrophy and affects 1 in approximately 4000 male births. Mutations in the dystrophin gene on chromosome Xp21 result in the absence of the 427 kD protein dystrophin, a key component in a complex of proteins that connects the cytoskeleton to the extracellular matrix. The

lack of dystrophin leads to mechanical instability of the cell membrane (Gailly, 2002) and renders it more susceptible to rupture (Petrof *et al.*, 1993), causing elevated Ca^{2+} influx and increased susceptibility to oxidative stress (Lawler, 2011), which activate each other in a vicious cycle that contributes to DMD pathogenesis. Several studies have suggested that the rise in intracellular Ca^{2+} is an important initiating event in the pathogenesis of dystrophic muscle (Whitehead *et al.*, 2006; Hopf *et al.*, 2007; Millay *et al.*, 2009). The increased Ca^{2+} entry occurring during activity, particularly during eccentric exercise, may lead to local proteolytic activation of cationic channels and result in a further increase of Ca^{2+} entry (Alderton and Steinhardt, 2000). Stretch-activated channels (SACs) and store-operated channels (SOCs) are regarded as candidates for this excessive Ca^{2+} influx (Ruegg *et al.*, 2012). Physiological and pharmacological data indicate that these channels belong to the same channel population or share common constituents (Ducret *et al.*, 2006). Earlier work from our laboratory and others' showed that SOCs and SACs are regulated, at least in part, by the Ca^{2+} independent form of PLA_2 ($iPLA_2\beta$; Boittin *et al.*, 2006; Bolotina, 2008; Burkholder, 2009). PLA_2 activity has been shown to be up to 10-fold higher in muscles from DMD patients compared with normal controls (Lindahl *et al.*, 1995). Muscles from mdx^{5Cv} mice, a mouse model for DMD, also showed increased $iPLA_2$ expression (Boittin *et al.*, 2006). All these findings led to the hypothesis that inhibition of $iPLA_2$ would reduce the excessive Ca^{2+} entry and ameliorate the pathogenesis of DMD.

The anthracycline antibiotic doxorubicin (Dox) and its congener, daunorubicin, have been used since the 1970s to treat a variety of malignancies, including leukaemias, lymphomas and solid tumours (Gaitanis and Staal, 2010). Their anti-tumour effect has been attributed to intercalation between DNA strands (Jung and Reszka, 2001). The use of Dox and its analogues is limited by their cardiac toxicity. Swift and collaborators linked this to their ability to inhibit $iPLA_2$ (McHowat *et al.*, 2001; 2004; Swift *et al.*, 2003; 2007). Dox showed selectivity towards $iPLA_2$, the same enzyme that activates the Ca^{2+} channels thought to be involved in DMD pathogenesis. Dox-mediated inhibition of $iPLA_2$ was evident both *in vivo* and *in vitro* at clinically relevant concentrations as low as 100 nM.

We demonstrate here that Dox directly inhibits purified $iPLA_2$. Furthermore, Dox potently inhibits $iPLA_2$ activity in dystrophic myotubes and blocks SAC-mediated, but not SOC-mediated, Ca^{2+} influx, affecting Ca^{2+} handling and production of reactive oxygen species (ROS). Using isolated fast and slow dystrophic muscles, we found that Dox was not deleterious to force production and promoted recovery from eccentric contractions.

Methods

Cell culture

Myotubes were prepared from EDL-MDX-2 myoblasts as described previously (Wagner *et al.*, 2003; Basset *et al.*, 2004). Briefly, myoblasts were plated on collagen-treated Petri dishes (Falcon; Becton Dickinson, Heidelberg, Germany) in a proliferation medium containing a 1:1 mixture of Dulbecco's modified minimal essential medium (DMEM; Invitrogen, Karlsruhe, Germany) with 4.5 $g \cdot L^{-1}$ glucose and MCBD202 (supplemented with $NaHCO_3$ and 1% v/v Glutamax II x100; Gibco, Paisley, UK), 10% FBS (Invitrogen, Zug Switzerland), 1% Ultroser SF (BioSepra, Saint-Christophe, Cergy, France) and 10 $\mu g \cdot mL^{-1}$ ciprofloxacin (Bayer, Leverkusen, Germany). The myoblasts were cultured on a feeder layer of 10T½ fibroblasts to support the growth and viability of the muscle cells (Pinset *et al.*, 1991). Briefly, the 10T½ fibroblasts were inactivated for 4 h with mitomycin C (2 $\mu g \cdot mL^{-1}$; Sigma, Buchs, Switzerland) in DMEM containing 10% FBS and 10 $\mu g \cdot mL^{-1}$ ciprofloxacin. Cells were then seeded in the same proliferation medium as above at densities of 40 000 EDL-MDX-2 myoblasts and 30 000 inactivated fibroblasts per well in 24-well plates coated with 1 $\mu g \cdot cm^{-2}$ Matrigel (Becton Dickinson). After 2 days, myotube formation was induced by changing the medium to a differentiation medium consisting of 1:1 v/v DMEM and MCDB202 medium, supplemented with 1.7% FBS, 3.3% horse serum (Invitrogen), 10 $\mu g \cdot mL^{-1}$ insulin (Sigma) and 10 $\mu g \cdot mL^{-1}$ ciprofloxacin. After 3–4 days, mature contracting myotubes were obtained.

C2C12 myoblasts were plated in 24-well plates at a density of 30 000 cells per well in DMEM supplemented with 10% FBS and 10 $\mu g \cdot mL^{-1}$ ciprofloxacin. When 60–80% confluent, myotube formation was induced by switching to differentiation medium (DMEM containing 2% horse serum and ciprofloxacin as above). Four days later, the cultures were used for the experiments.

Determination of PLA_2 activity

PLA_2 activity was measured using a cell-permeant fluorescent probe, PED-6 (Invitrogen). PED-6 is cleaved by PLA_2 to release BODIPY, a green fluorescent compound. The measured fluorescence is proportional to PLA_2 activity. Briefly, EDL-MDX-2 myotubes on a layer of 10T½ fibroblasts or C2C12 myotubes were washed with a calcium-free physiological salt solution (PSS; composition in mM: HEPES, 5; KCl, 5; $MgCl_2$, 1; NaCl, 145; glucose, 10 and EGTA, 0.2) to promote activation of $iPLA_2$. PED-6 (1 μM) was added and the fluorescence increment was measured over a period of 30 min at 37°C using a FLUOStar Galaxy fluorimeter (BMG Laboratories, Offenburg, Germany) set for measurements every 15 s with an excitation wavelength of 488 nm and emission at 520 nm (Reutenauer-Patte *et al.*, 2012).

Cloning of mouse $iPLA_2\beta$ into expression plasmid

A pCMV6-Kan/Neo vector containing the mouse $iPLA_2\beta$ transcript variant 1 (Ref. MC202080, TrueClone; OriGene, Rockville, MD, USA) was used for cloning the full-length mouse $iPLA_2\beta$ cDNA and inserting 6x histidine (His) tags in a pAAV-CMV-MCS expression vector (Ref. VPK-410-SER2, Cell Biolabs, Lucerne, Switzerland). Briefly, the full-length mouse $iPLA_2\beta$ cDNA was amplified by PCR using the high-fidelity Phusion DNA polymerase (New England Biolabs, Ipwich, UK) and primers (Microsynth, Balgach, Switzerland) designed for inserting SalI and BglII restriction sites, as well as a 6x His tag with a short-flexible Gly-Ser linker at either the N-terminus (primers 372Fwd + 372Rev) or the C-terminus (primers 373Fwd + 373Rev): primer 372Fwd: 5′-ATG CAG TCG ACA TGC ATC ATC ACC ATC ACC ACG GCA GCC AGT TCT TCG GAC GCC TCG-3′; primer 372Rev: 5′-ATG CAA GAT CTT

CAG GGA GAC AGC AGC AGC TGG-3′; primers 373Fwd: 5′-ATG CAG TCG ACA TGC AGT TCT TCG GAC GCC T-3′; primers 373Rev: 5′-ATG CAA GAT CTT CAC TAG TGG TGA TGG TGA TGA TGG CTG CCG GGA GAC AGC AGC AGC TGG-3′. The SalI- and BglII-digested PCR products were gel-purified and ligated into dephosphorylated SalI- and BglII-digested pAAV-CMV-β-globin intron-MCS expression vector. Competent *Escherichia coli* were transformed, positive clones were selected and sequence identity were verified (Fasteris SA, Plan-les-Ouates, Switzerland) by classical procedures. The vectors pITER #63 (pAAV-CMV-N_{His}-iPLA$_2$β) and pITER #64 (pAAV-CMV-C_{His}-iPLA$_2$β) were selected for further expression and purification steps.

Expression and purification of recombinant mouse iPLA$_2$β

HEK293 cells cultured in six-well plates were transfected when about 60% confluent with pITER #63 or pITER #64 using Lipofectamine 2000 (Life Technologies, Zug, Switzerland) according to the provider's recommendations. HEK293 cells transfected with pITER#10 (pAAV-CMV vector expressing the red fluorescent reporter DsRedExpress2) were used to monitor the efficacy of the transfection. About 44 h post-transfection, the supernatant was discarded, cells were gently scrapped in ice-cold lysis buffer (20 mM sodium phosphate, 10% glycerol, pH 7.8), 800 µL per well. Cells were broken by passing them 10 times through a 26-G needle, and the suspension was sonicated. After centrifugation at 10 000× *g* for 20 min at 4°C, the clarified supernatants were loaded onto a 1 mL HisTrap FF column (GE Healthcare Life Sciences, Glattbrugg, Switzerland) loaded with nickel, washed with buffer A (20 mM sodium phosphate, 500 mM NaCl, 10% glycerol, pH 7.8) containing 4% buffer B (20 mM sodium phosphate, 500 mM NaCl, 500 mM imidazole, 10% glycerol, pH 7.8) and finally eluted using a gradient of 4 to 100% buffer B (10 column volumes) with a flow rate of 1 mL·min^{-1}. The PLA$_2$ activity in the fractions was assayed using PED-6 as above. The fractions showing the highest activity were pooled. Aliquots of the homogenates and of the fractions collected during the purification process were resolved by SDS-PAGE using gradient gels containing 6% acrylamide and 0% glycerol (top) to 11% acrylamide and 10% glycerol (bottom) and with 10 mM 2-mercaptoethanol in the cathode chamber. Coomassie Blue staining and immunoblotting with a rabbit polyclonal antibody raised against iPLA$_2$β (Cayman Chemicals, Ann Arbor, MI, USA) were performed according to classical procedures to check the purity and identity of N_{His}-iPLA$_2$β and C_{His}-iPLA$_2$β.

Determination of ROS production

Oxidative stress was measured using DCFH-DA (Invitrogen), a probe for ROS that readily enters cells, becomes deacetylated into the non-fluorescent membrane impermeant DCFH, which can react with a variety of reactive oxygen/nitrogen species, such as hydrogen peroxide, superoxide and peroxynitrite, to yield dichlorofluorescin (DCF$^-$), a fluorescent compound. Following our procedure (Dorchies *et al.*, 2009), cells were washed twice with PSS– and incubated with 20 µM of DCFH-DA in PSS– for 1 h to allow sufficient loading of the cells. Subsequently, compounds to be tested were added and the development of the fluorescent signal was monitored with a FLUOStar Galaxy fluorimeter, as described above.

$^{45}Ca^{2+}$ influx under conditions of store depletion and hypo-osmotic shock

$^{45}Ca^{2+}$uptake was recorded as described by Passaquin *et al.* (1998), with minor modifications. To quantify SAC activity, myotube cultures were washed twice with PSS containing 1.2 mM Ca^{2+} (PSS+), pre-incubated at 37°C for 15 min with test compounds and then exposed to a hypo-osmotic PSS+ (100 mOsm obtained by decreasing the NaCl concentration from 145 to 25 mM) containing 1 µCi·mL^{-1} of $^{45}Ca^{2+}$. Such a procedure has been shown to cause myotube swelling, distension of the plasma membrane and opening of SAC (Fanchaouy *et al.*, 2009). Ca^{2+} influx was stopped by placing the cultures on ice and washing four times with 0.5 mL of ice-cold PSS–. Cells were subsequently lysed with 0.5 mL of 1 N NaOH, and the radioactivity in the lysates was determined by scintillation counting (Ultima Gold, Packard, Groningen, The Netherlands) using a beta-counter (LKB Wallac 1217 Rackbeta, Turku, Finland).

To study SOC activity, a protocol similar to that used on isolated fibres (Boittin *et al.*, 2006) was employed with slight modifications. Briefly, myotube cultures were washed twice with PSS–, pre-incubated for 15 min at 37°C in 200 µL PSS–, and finally exposed for 15 min to PSS– containing the test compounds and 5 µM thapsigargin to ensure complete depletion of the intracellular Ca^{2+} stores. Calcium influx was initiated by switching to PSS+ containing 1 µCi·mL^{-1} $^{45}Ca^{2+}$ and the test compounds. After 10 min, cells were washed, lysed and the radioactivity was determined as above.

Measurement of subsarcolemmal Ca^{2+} concentrations

Myoblasts were transfected with plasmids allowing targeted expression of the Ca^{2+}-sensitive photoprotein aequorin at the plasma membrane, as described previously (Basset *et al.*, 2004). Briefly, 80 000 EDL-MDX-2 myoblasts were seeded on 13-mm-diameter Thermanox coverslips (Nalge Nunc International, Penfield, NY, USA) in four-well plates. When 80–90% confluent, growth medium was removed and transfection was carried out as described above. On the next day, the cells were placed in differentiation medium to induce myotube formation as above. The plasmids were pcDNAI expression vectors containing the wild-type aequorin coding sequence fused with the plasma membrane-targeting sequence from SNAP-25 for measurements of subsarcolemmal Ca^{2+}concentrations (Rizzuto *et al.*, 1992).

Subsarcolemmal Ca^{2+} concentrations were determined after 3–4 days of differentiation. Briefly, myotubes were exposed to 5 µM coelenterazine (Calbiochem, Darmstadt, Germany) for 1 h, and then superfused at a rate of 3 mL·min^{-1} in a custom-made 0.5 mL chamber at 37°C (MecaTest, Geneva, Switzerland). Emitted luminescence was recorded every second with single photon-counting tubes (EMI 9789A, Electron Tubes Ltd, Uxbridge, UK) using a computer with a photon-counting board (EMI C660). Signal calibration was carried out by permeabilizing cells with 100 µM digitonin in the presence of 10 mM $CaCl_2$ in order to consume all remaining aequorin. The increment in maximum amplitude upon exposure to hypo-osmotic shock was calculated in the presence and absence of Dox, or *S*-bromoenol lactone (*S*-BEL), a selective inhibitor of iPLA$_2$.

Isolated muscle experiments

To evaluate whether Dox affects skeletal muscle performance, a modification of the method described by Brooks & Faulkner (1988) was used. Dystrophic (mdx^{5Cv}) and wild-type (C57BL/6J) mice were maintained in the animal facility of the School of Pharmaceutical Sciences and used in compliance with the local rules on animal experimentation and welfare (Authorization #106/3626/0 delivered by the Cantonal Veterinary Office of Geneva and approved by the Swiss Veterinary Office). Mice between 8 and 12 weeks of age were anaesthetized, the extensor digitorum longus muscle (EDL) and soleus muscles (SOL) were exposed, and their proximal and distal tendons were tied with silk sutures. The proximal tendons were tied to an isometric force transducer (Hugo Sachs Elektronik, Hugstetten, Germany), and the distal tendons fixed to a pin in vertical incubation chambers (Radnoti, Monrovia, CA, USA) filled with a physiological Ringer solution (composition in mM: NaCl, 137; $NaHCO_3$, 24; glucose, 11; KCl, 5; $CaCl_2$, 2; $MgSO_4$, 1; NaH_2PO_4, 1; and d-tubocurarine chloride, 0.025) continuously bubbled with 95% O_2–5% CO_2. Muscles were stimulated by 0.2 ms square wave pulses generated by a Grass S88X stimulator (Grass Technologies, West Warwick, RI, USA) delivered via platinum electrodes on both sides of the muscles. After setting the optimum stimulating voltage and the optimum length (L_0), muscles were divided into two experimental groups. The first group served to evaluate the force and kinetics of contraction and relaxation before and after treatment with test compounds. After addition of vehicle to the bathing solution, a series of three phasic twitches was recorded. Then, the force-frequency dependency was established by delivering 500 ms long pulses of increasing frequency (50, 100 and 150 Hz). Finally, after incubation with the compounds for 20 min, the procedure was repeated. The phasic twitch traces were used to determine the absolute phasic tension, the time-to-twitch-peak tension and the time for half-relaxation from the twitch peak. Muscles in the second group were exposed to vehicle or test compounds for 20 min prior to being subjected to two stimulation protocols of different intensity aimed at inducing two types of fatigue: The 'mild-intensity protocol' consisted of 20 tetanic stimuli at 100 Hz for a duration of 200 ms, with 30 s rest between contractions, and the 'high-intensity protocol' consisted of 60 tetanic stimuli at 80 Hz (EDL) or 60 Hz (SOL), for a duration of 1 s every 4 s. The change in muscle tension as the stimulations were repeatedly delivered was expressed as a percentage of the tension generated by the first stimulation. In another set of experiments, EDL muscles were placed in a 10 mL horizontal chamber in an eccentric muscle test system, model 305C-LR (Aurora Scientific Inc., Aurora, ON, Canada). The optimum stimulating voltage and L_0 were set and EDL muscles were exposed to 10 contractions of 400 ms each at 100 Hz, 30 s apart. One hundred and fifty milliseconds after the initiation of each contraction, the muscle was stretched by a value of 9% of L_0 over a period of 100 ms at a speed of 0.9 $L_0 \cdot s^{-1}$ and maintained at that level for another 100 ms before returning to the original length at the end of the stimulation. Force loss and recovery after 20 min of rest were expressed for every muscle.

Statistics

Results are reported as mean ± SEM. Comparisons within each experiment were analysed by one-way ANOVA followed by Dunnett's multiple comparison post-tests using the GraphPad Prism software, version 5 (GraphPad Software, La Jolla, CA, USA). Differences were considered significant at values of $P \leq 0.05$.

Results

We tested the hypothesis that Dox inhibits $iPLA_2$ in normal and dystrophic skeletal muscle cells and explored the consequences of Dox treatment on intracellular Ca^{2+} handling and muscle performance.

Doxorubicin inhibits PLA_2 activity in C2C12 and dystrophic myotubes

C2C12 cells grown into myotubes were used to evaluate the inhibitory effect of Dox on PLA_2. Experiments were carried out in the absence of Ca^{2+} and in the presence of 0.2 mM EGTA (PSS–) to chelate Ca^{2+} and maximize the contribution of $iPLA_2$ over other Ca^{2+}-dependent isoforms (Reutenauer-Patte *et al.*, 2012). Dox showed a concentration-dependent inhibition starting at 1 μM, and reaching a value of 33.0 ± 3.2% of non-treated cells at 60 μM as depicted in Figure 1. Dox was as potent as the most commonly used inhibitor for $iPLA_2$, *S*-BEL, at the same concentration of 30 μM. The inhibition exerted by the general PLA_2 inhibitor methyl arachidonyl fluorophosphonate (MAFP) was greater than that of the $iPLA_2$-specific inhibitor *S*-BEL and the $cPLA_2$ selective inhibitor arachidonyl trifluoromethyl ketone ($AACOCF_3$). Thus, our results suggest that Dox preferentially inhibits $iPLA_2$, in accordance with previous data (Swift *et al.*, 2007).

We obtained similar results using EDL-MDX-2 dystrophic myotubes, our model cells for DMD. Dox at concentrations of 1–60 μM resulted in a reduction of the PED-6 signal down to 50.6 ± 9.5% of control activity (n = 5–9). Again, when compared with *S*-BEL and $AACOCF_3$, Dox at 30 μM showed similar potency (Figure 1C).

Doxorubicin inhibits purified $iPLA_2\beta$ through a direct interaction

Transfection of HEK293 cells with pITER #63 or pITER #64 resulted in overexpression of the N_{His}-$iPLA_2\beta$ or C_{His}-$iPLA_2\beta$, respectively, to levels comparable to that of the control reporter gene *DsRedExpress2* (Figure 2A, B). After lysis, both 6x His-tagged $iPLA_2\beta$ enzymes present in the soluble fraction were nickel-affinity purified, yielding pure enzyme (Figure 2A, B). Using the pure C_{His}-$iPLA_2\beta$, Dox showed a concentration-dependent inhibition with an IC_{50} value of around 16.5 μM (Figure 2C, D). Dox at 30 μM was as potent as the classical inhibitors *S*-BEL and MAFP used in the same concentration range.

Although the method described here resulted in the production of pure enzymes from the soluble fractions, the majority of the overexpressed $iPLA_2\beta$ was found in the insoluble fractions of the homogenates, likely because of $iPLA_2\beta$ aggregation through their ankyrin repeats (Hsu *et al.*, 2009). In an attempt to recover the $iPLA_2\beta$ protein, the pellets were washed with a buffer containing 20 mM sodium phosphate, 134 mM NaCl, 10% glycerol and 1% *n*-octyl-β-D-glucopyranoside at pH 7.8, which removed most contami-

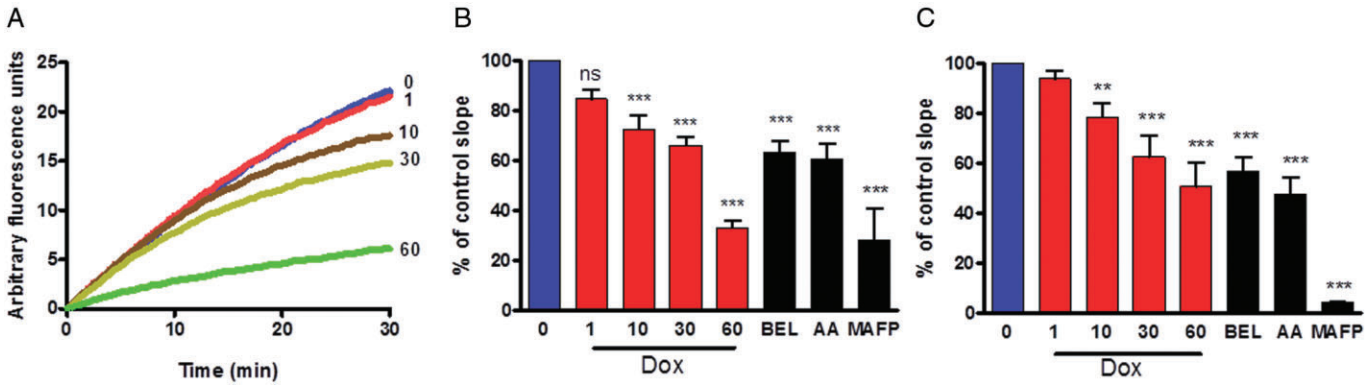

Figure 1

Assessment of Dox effect on $iPLA_2$ activity in normal and dystrophic myotubes. PED-6 was used to measure the activity of PLA_2 in C2C12 and EDL-MDX-2 myotubes. Measurements were made in PSS devoid of Ca^{2+} and in the presence of 0.2 mM EGTA (PSS–) in order to chelate Ca^{2+} and maximize the contribution of $iPLA_2$ over other isoforms. Cells were incubated with test compounds at the indicated concentrations (μM) for 20 min prior to the measurements (n = 3–14). The inhibitory effect was compared with one of the selective $iPLA_2$ inhibitor, *S*-BEL (30 μM), a selective $cPLA_2$ inhibitor, $AACOCF_3$ (AA, 50 μM) and with the global PLA_2 inhibitor, MAFP (25 μM). (A) Representative traces in C2C12 myotubes showing fluorescence increments over time resulting from the cleavage of PED-6 by cellular PLA_2 and its inhibition by increasing concentration of Dox (μM). (B) PLA_2 activity in C2C12 myotubes. (C) PLA_2 activity in EDL-MDX-2 myotubes. *$P \leq 0.05$; **$P \leq 0.01$; ***$P \leq 0.001$.

nants. After centrifugation as above, the resulting pellets were resuspended in lysis buffer and analysis revealed nearly pure $iPLA_2\beta$ (Figure 2A, B). Both the pellet-purified and the soluble fraction-purified C_{His}-$iPLA_2\beta$ showed the same sensitivity to Dox and to PLA_2 inhibitors (not shown).

Doxorubicin exhibits a biphasic effect on ROS production in dystrophic myotubes

We investigated whether Dox affects ROS production in dystrophic skeletal muscle cells under conditions that maximize $iPLA_2$ activity. Dox caused a concentration-dependent increase in ROS production, amounting to twofold at 30 μM in the first 10 min. This rise was followed by an inhibition of the activity down to 77.0 ± 5.1% of control activity over the following 20 min (Figure 3). *S*-BEL had no effect, suggesting that $iPLA_2\beta$ did not affect ROS production.

Doxorubicin inhibits $^{45}Ca^{2+}$ influx through SAC but not SOC

To study a potential effect of Dox on SAC, differentiated myotubes were subjected to a hypo-osmotic buffer, a procedure used to induce swelling and subsequent opening of SAC. After 5 min under hypo-osmotic conditions, $^{45}Ca^{2+}$ influx increased to a value of 252.6 ± 14.0% when compared with myotubes kept in an isotonic buffer. Dox at a concentration as low as 1 μM inhibited stretch-induced influx to an extent similar to that of 300 μM streptomycin or 30 μM of the spider venom peptide GsMTx4, the most commonly used and specific SAC inhibitors (Whitehead *et al.*, 2006) or to 30 μM *S*-BEL (Figure 4A).

$^{45}Ca^{2+}$ influx via thapsigargin-stimulated SOC was increased to a value of 354.6 ± 26.3% compared with controls. Dox at concentrations up to 30 μM had no significant effect on SOC influx. Treating the cells with *S*-BEL or with the SOC blocker, BTP2 (Zitt *et al.*, 2004; Boittin *et al.*, 2006) resulted in about 90% inhibition (Figure 4B).

Dox alters subsarcolemmal Ca^{2+} under hypo-osmotic conditions

Muscle fibres or cultured myotubes prepared from dystrophic mice have been shown to display a 4- to 10-fold increase of Ca^{2+} in the narrow space underneath the sarcolemma, as compared to wild-type cells when analysed using the Ca^{2+}-sensitive photoprotein aequorin targeted to this space (Basset *et al.*, 2004). We used transfected muscle cells expressing aequorin restricted to this space.

Superfusing the myotubes with a hypo-osmotic buffer resulted in an increase of the maximum amplitude of subsarcolemmal Ca^{2+} with a value of 3.01 ± 0.23 μM, while myotubes in normo-osmotic PSS+ remained at around 1.5 μM (Figure 5). Incubation with 10 or 30 μM Dox prior to and during the hypo-osmotic shock limited this increase to a value of 1.66 ± 0.35 and 1.47 ± 0.13 μM, respectively, corresponding to about a 50% reduction of the stretch-induced Ca^{2+} elevation in the sub-sarcolemmal space. Interestingly, *S*-BEL produced no significant effect.

Dox affects fatigability and recovery from eccentric contraction but not force production of isolated muscles

In experiments using isolated muscle, a concentration of 30 μM Dox was used, as this concentration showed efficacy on PLA_2 activity, ROS production and Ca^{2+} handling in cellular assays. To investigate the acute Dox effects on dystrophic muscle contraction parameters, we chose the EDL and the SOL muscles as models for the fast-contracting, fatigue sensitive muscles and slow-contracting, fatigue insensitive muscles respectively.

Acute treatment of EDL and SOL muscles with 30 μM Dox had no effect on either absolute phasic or tetanic forces (Figure 6). Neither did Dox have any effect on the kinetics of contraction, as evaluated by the time-to-peak and the time for half-relaxation from the peak.

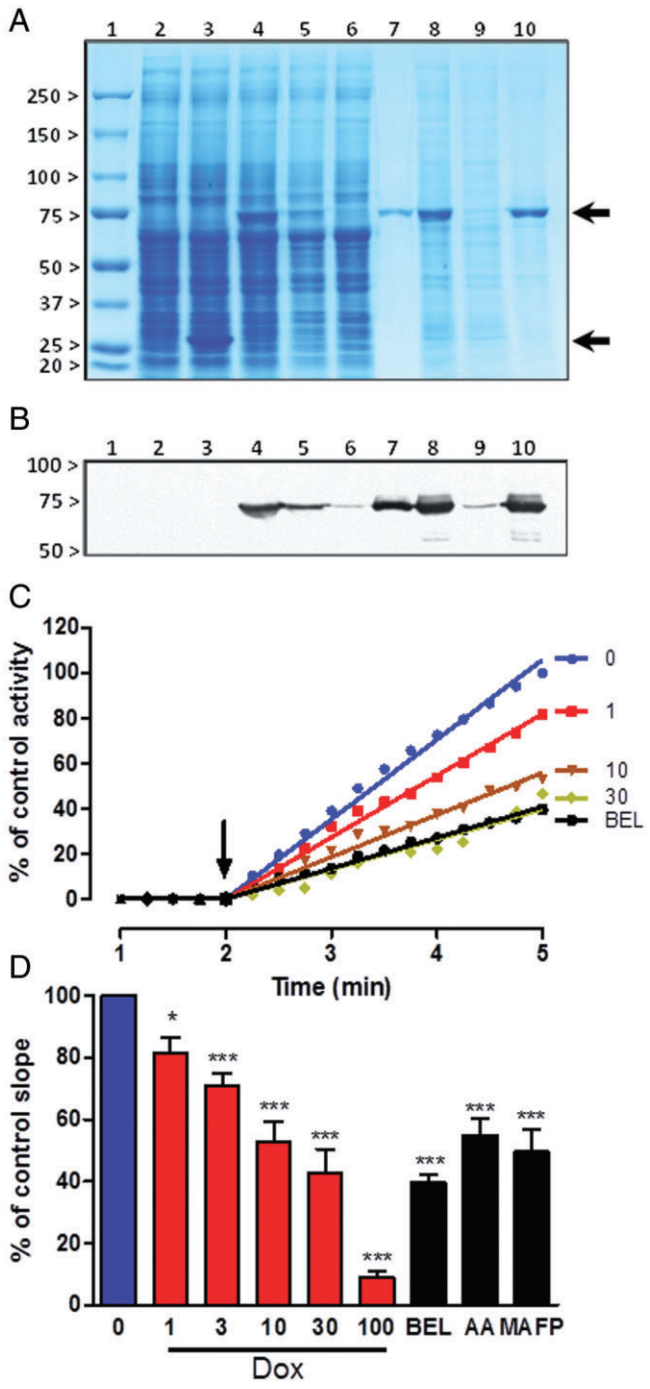

Figure 2

Inhibitory action of Dox on purified recombinant mouse iPLA$_2$β. Histidine-tagged iPLA$_2$β was overexpressed in HEK293 cells, purified by nickel-affinity chromatography and used to assay the ability of Dox to inhibit iPLA$_2$β activity through direct interaction. (A) Coomassie-stained gels, (B) Western-blot detection of iPLA$_2$β. Molecular weight markers (lane 1; in kDa). Homogenates from non-transfected cells (lane 2), cells overexpressing DsRedExpress2 (lane 3) or cells overexpressing C_{His}-iPLA$_2$β (lane 4) were prepared in lysis buffer. The overexpressed DsRedExpress2 and C_{His}-iPLA$_2$β are shown by arrows at around 25 and 80 kDa respectively. After centrifugation, the soluble fraction of the C_{His}-iPLA$_2$β overexpressing cell lysate (lane 5) was loaded on a nickel column. The flow-through (lane 6) was depleted from C_{His}-iPLA$_2$β and pure C_{His}-iPLA$_2$β was eluted from the nickel column (lane 7). The insoluble fraction (pellet) still contained most of the overexpressed C_{His}-iPLA$_2$β (lane 8). Washing the pellet with *n*-octyl-β-D-glucopyranoside removed most contaminants (lane 9) and yielded nearly pure C_{His}-iPLA$_2$β that was readily recovered by centrifugation (lane 10). Protein obtained from the purified pellet was active and displayed the same sensitivity to Dox and classical PLA$_2$ inhibitors as the enzyme purified from the soluble fraction. (C) Traces (average of 4–8 determinations) showing the inhibition of pure C_{His}-iPLA$_2$β by increasing concentrations of Dox (μM) and by *S*-BEL (30 μM) using the fluorogenic substrate PED-6, which was added at the time indicated by the arrow. (D) Quantification of the inhibitory effect of the tested compounds at the indicated concentrations (μM) on C_{His}-iPLA$_2$β activity (n = 4–8) and its comparison to the classical inhibitors MAFP (25 μM) and AACOCF$_3$ (AA, 50 μM). ***$P \leq 0.001$. See text for details.

In order to investigate the effects of Dox on fatigue, EDL and SOL muscles were consecutively exposed to two regimens of repeated tetanizations. When exposed to the mild-intensity protocol, SOL muscles did not lose force up to the 20th cycle, whereas the force of the dystrophic EDL muscles declined to 88.5 ± 2.0% of the initial values. This muscle fatigue was completely recuperated after 5 min of rest. Treating the EDL or SOL dystrophic muscle with 30 μM Dox did not affect their fatigability, whereas *S*-BEL treatment (30 μM) almost doubled the rate of force loss, yielding a force of 77.4 ± 3.7% of the initial values after only 20 mild contractions (Figure 7A).

Dystrophic EDL muscle exposed to the high-intensity fatigue protocol showed a primary phase of potentiation of the force to a value of 30% above the initial force during the first 10 contractions before the force loss phase commenced. Treatment of the muscles with either Dox or *S*-BEL abolished the potentiation phase (Figure 7B). When SOL muscles were exposed to drastic fatigue, they displayed a pattern resembling that of mildly fatigued EDL. Non-treated dystrophic SOL muscles showed a decline of force to a value of 68.9 ± 2.8% of the initial values. Dox treatment caused a deterioration of muscle performance reaching a value of 60.6 ± 5.8% of initial values, similar to *S*-BEL, which attained a value of 60.8 ± 5.1% (Figure 7C).

To further explore the effects of Dox on muscle function, EDL muscles were exposed to a series of 10 eccentric contractions, that is, tetanic contractions during which the muscles were stretched in a direction opposite to the contraction. Such lengthening contractions are known to be particularly deleterious to dystrophic muscles. In this assay, wild-type EDL muscle lost 30% of its initial force while dystrophic EDL lost around 40% (Figure 8A). Dox treatment did not cause further loss of force in dystrophic muscles. *S*-BEL, however, showed a significant deleterious effect since the force declined down to 42.2 ± 5.7%. After a 20 min recovery period, wild-type muscles showed a marked recovery of 13.47 ± 1.0% of their pre-contraction value, while dystrophic muscle recuperated only slightly (by 2.7 ± 2.6%). Dox-treated muscles recovered with a value of 11.6 ± 2.6%, while those treated with *S*-BEL displayed further deterioration of force during the recovery period, losing an additional 6.8 ± 3.7% (Figure 8B).

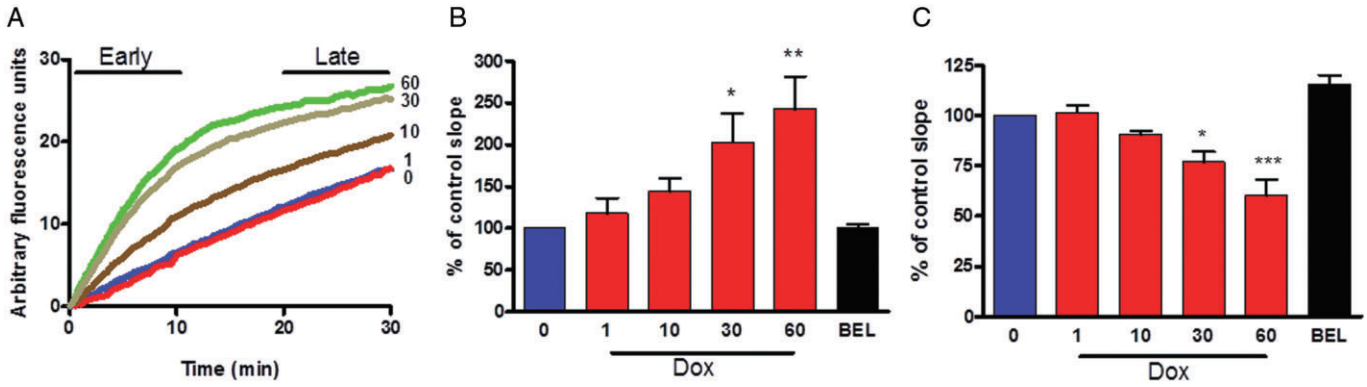

Figure 3

Modulation of ROS production by Dox in dystrophic myotubes. The probe DCFH-DA was used to monitor ROS production in EDL-MDX-2 myotubes. Cells were incubated with the probe for 1 h prior to measurement in order to allow deacetylation and trapping of the probe. Test compounds were added at the indicated concentrations (μM) and fluorescence increments monitored over 30 min. (A) Representative traces in EDL-MDX-2 myotubes showing fluorescence increment over time resulting from the oxidation of DCFH by free radicals and its inhibition by increasing concentrations of Dox (μM). (B) Early phase (0–10 min) effect of Dox compared to control and 30 μM *S*-BEL. (C) Late phase (20–30 min), n = 6–8 for (B) and (C). *$P \leq 0.05$; **$P \leq 0.01$; ***$P \leq 0.001$.

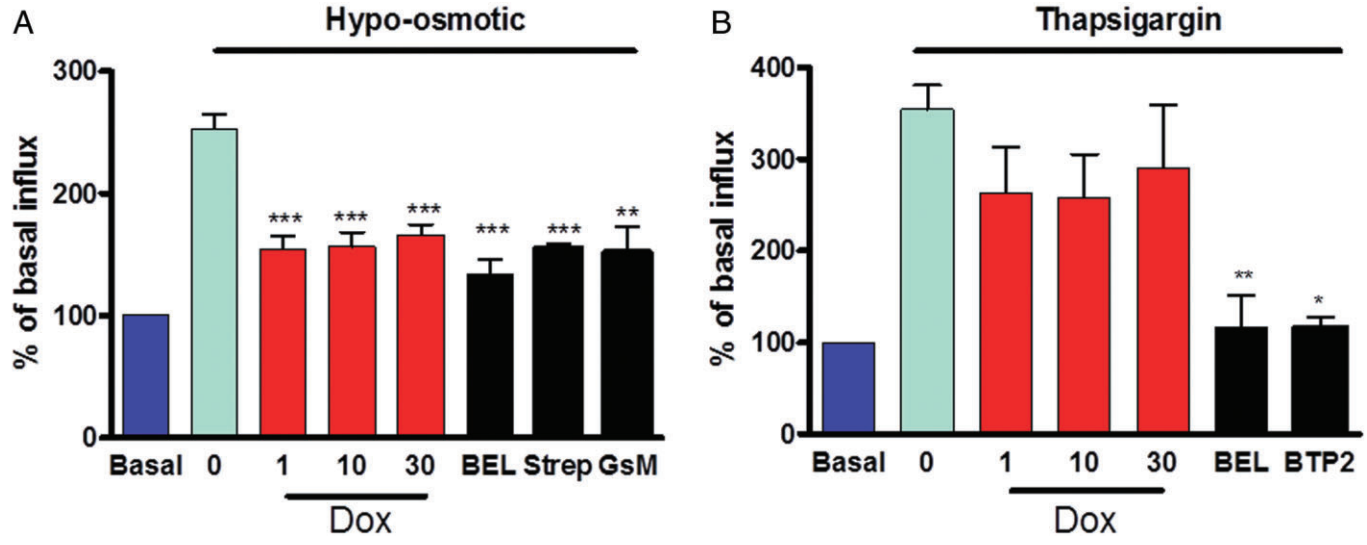

Figure 4

Effect of Dox on hypo-osmotic- and thapsigargin-induced $^{45}Ca^{2+}$ influx. $^{45}Ca^{2+}$ was used to measure influx under conditions of hypo-osmotic shock (A) or in the presence of 5 μM thapsigargin (B) in EDL-MDX-2 myotubes. Cells were treated with 300 μM of streptomycin or 30 μM GsMTx4 (GsM), inhibitors of SAC, 10 μM BTP2, an inhibitor of SOC, 30 μM *S*-BEL, an inhibitor of iPLA$_2$β, or Dox at the indicated concentrations in μM (n = 3–15). *$P \leq 0.05$; **$P \leq 0.01$; ***$P \leq 0.001$.

Discussion

In the current study, we report that Dox inhibits iPLA$_2$ activity in both wild-type and dystrophic skeletal muscle cells. Moreover, using the purified recombinant enzyme, we demonstrated, for the first time, that Dox is able to directly inhibit iPLA$_2$β activity. Using a combination of assays, we also demonstrated the ability of Dox to inhibit Ca^{2+} influx through SAC, but not SOC, to modulate ROS production, alter fatigability and ameliorate the post-traumatic recovery of dystrophic muscles. Overall, our findings suggest that these effects resulted from both direct and indirect inhibition of iPLA$_2$β by Dox. A possible model showing the sites of action of Dox on these pathways is shown in Figure 9.

The ability of Dox to inhibit iPLA$_2$ activity in skeletal muscle cells is in accordance with earlier reports on cardiomyocytes (McHowat *et al.*, 2001; Swift *et al.*, 2003; 2007). Dox showed a similar potency towards iPLA$_2$ as *S*-BEL, currently the most potent and selective inhibitor of this enzyme. BEL is a suicide inhibitor, which covalently binds and irreversibly inhibits iPLA$_2$ (Hazen *et al.*, 1991). To evaluate if Dox inhibited the enzyme directly, we cloned the full-length mouse

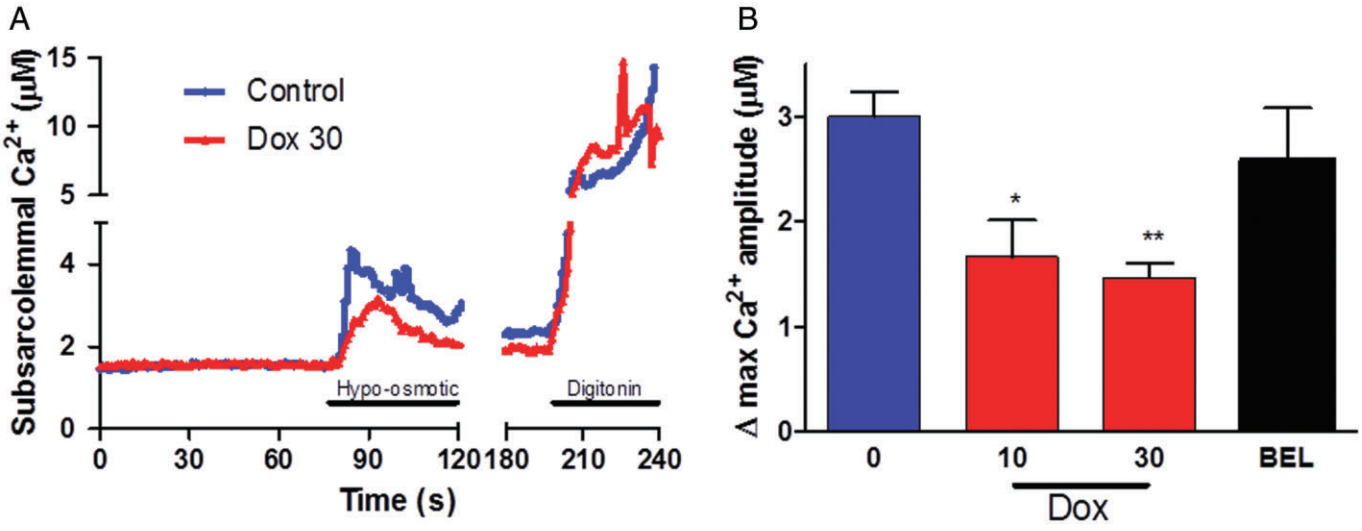

Figure 5

Effect of Dox on subsarcolemmal Ca^{2+} in response to hypo-osmotic shock. The bioluminescent protein aequorin was targeted to the subsarcolemmal space in order to measure the responses to hypo-osmotic shock. (A) Representative traces showing responses to hypo-osmotic shock of EDL-MDX-2 myotubes transfected with SNAP-25 aequorin, treated or untreated with 30 μM Dox. (B) Difference between maximal amplitudes reached in myotubes treated with vehicle, Dox or *S*-BEL (30 μM). $*P \leq 0.05$; $**P \leq 0.01$; $***P \leq 0.001$.

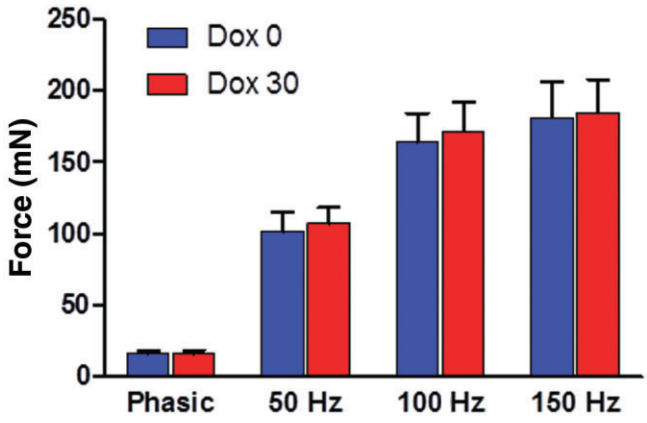

Figure 6

Dox does not affect force production in isolated dystrophic EDL muscle. EDL muscles were isolated from 8- to 12-week-old mdx^{5Cv} mice and maintained at their optimal length in oxygenated physiological buffer. A force-frequency relationship was established by electrical stimulation at 50, 100 and 150 Hz before and 20 min after treatment with 30 μM Dox (n = 5). Phasic twitches produced by single stimulation are shown for comparison.

$iPLA_2\beta$ and introduced a histidine tag to allow affinity purification. Dox inhibited the purified $iPLA_2\beta$ in our assays with an IC_{50} of about 16.5 μM, indicating direct mode of inhibition. Nevertheless, this finding does not rule out other indirect interactions that could take place in intact cells.

A well-known consequence of Dox action in cells is a reduction of the ATP pool. In fact, Dox has been shown to inhibit key metabolic enzymes, such as GAPDH and glucose-6-phosphate dehydrogenase, resulting in lowered ATP levels (Wolf and Baynes, 2006). $iPLA_2\beta$ possesses an ATP-binding pocket that is important for the enzymatic activity (Ackermann *et al.*, 1994) and ATP has been shown to stabilize the enzyme during purification (Balboa *et al.*, 1997). Therefore, one such indirect effect of Dox on $iPLA_2\beta$ could be due to lowered ATP levels.

What are the molecular bases for Dox-mediated alteration of ROS production?

We examined whether the reported effects of Dox on increasing ROS production in cardiac cells were also valid in skeletal muscle cells. Using DCFH-DA as a probe, we found that Dox had a biphasic effect on ROS production. A concentration-dependent increase in ROS production was evident immediately after adding Dox to the myotubes; it continued for 10 min. Thereafter, a slight apparent concentration-dependent inhibition of ROS production was observed (Figure 2).

The structure of Dox plays a major role in ROS production. Its quinone moiety undergoes redox cycling on flavoenzymes by electron transfer from these to Dox, thus reducing the quinone to the semiquinone. Subsequent electron transfer from this to oxygen results in the formation of superoxide and hydrogen peroxide, thereby reverting the semiquinone to quinone. This redox cycling continues until the system becomes anaerobic, at which point oxygen radical production decreases and semiquinone begins to accumulate (Gutierrez, 2000). This phenomenon was reported to occur in mitochondria (Davies and Doroshow, 1986), to be associated with NOS (Fu *et al.*, 2004) or with cytochrome P450 (Bartoszek, 2002). ROS could also originate from a reduction of Dox by ferric ion of the heme moieties of NOS or NADPH oxidases (NOX). This was demonstrated to occur by the reversal of this effect using NOX inhibitors, and from the protection of mice deficient in gp^{91phox}, the core protein of NOX2, from Dox-induced cardiotoxicity (Gilliam and St

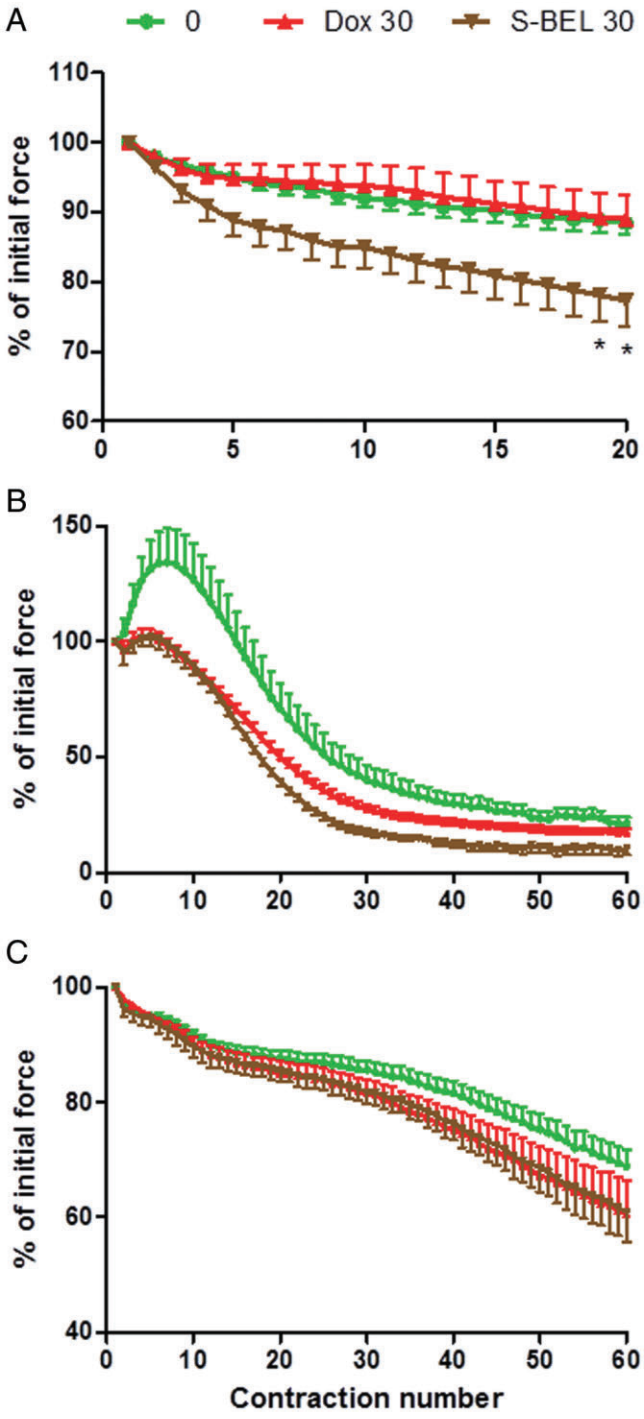

Figure 7

Treatment with Dox or *S*-BEL affects fatigue in isometrically contracting EDL and SOL dystrophic muscle. Isolated EDL and SOL muscles were fatigued using low- and high-intensity fatigue procedures. (A) Low-intensity fatigue in EDL muscles consisted of 20 contractions of 200 ms at 100 Hz, 30 s apart (n = 6–8). (B) High-intensity fatigue in EDL muscles consisted of 60 contractions of 1 s each at 80 Hz, repeated every 4 s (n = 5–11). (C) High-intensity fatigue in SOL muscle was carried out in the same manner as in EDL, but using 60 Hz instead of 80 Hz stimulations (n = 5).

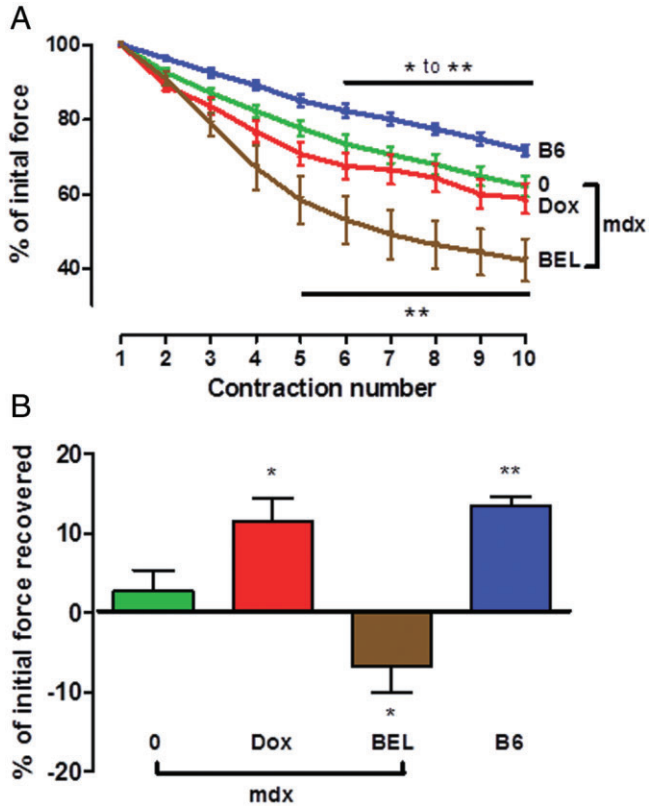

Figure 8

Eccentric contractions of EDL muscles reveal different responses to Dox and *S*-BEL. EDL muscles were exposed to 10 eccentric contractions of 400 ms at 100 Hz, 30 s apart. During each contraction, the muscle was stretched to 109% of its optimum length. (A) Responses of dystrophic, wild-type (B6), Dox (30 μM) and *S*-BEL (30 μM)-treated EDL muscles. Upper and lower lines show statistical significances between dystrophic and wild-type, dystrophic and *S*-BEL-treated EDL muscles, respectively. (B) Force recovered as % of pre-contraction force after a 20 min rest period showing enhanced recovery of wild-type muscles, restoration of normal recovery with Dox and further deterioration in muscles treated with *S*-BEL (n = 6–12). *$P \leq 0.05$; **$P \leq 0.01$; ***$P \leq 0.001$.

Clair, 2011). In relation to redox-generated ROS, the group of Sarvazyan postulated that Dox-mediated inhibition of $iPLA_2$ was due to oxidation of cysteine residues on the enzyme (McHowat *et al.*, 2001).

All of the above-mentioned mechanisms are likely to contribute to the increased ROS production seen in the early phase, while decreased ROS production in the late phase could be attributed to the system becoming anaerobic, or to depletion of co-factors.

Why does Dox cause SAC but not SOC inhibition?

The present report shows that Dox potently and completely inhibited Ca^{2+} influx through SAC but not SOC. In the past years, it has been established that SOC activity is mostly dependent on STIM1–Orai interactions (Cahalan, 2009), and that $iPLA_2\beta$ plays a role in modulating SOC activity (Boittin

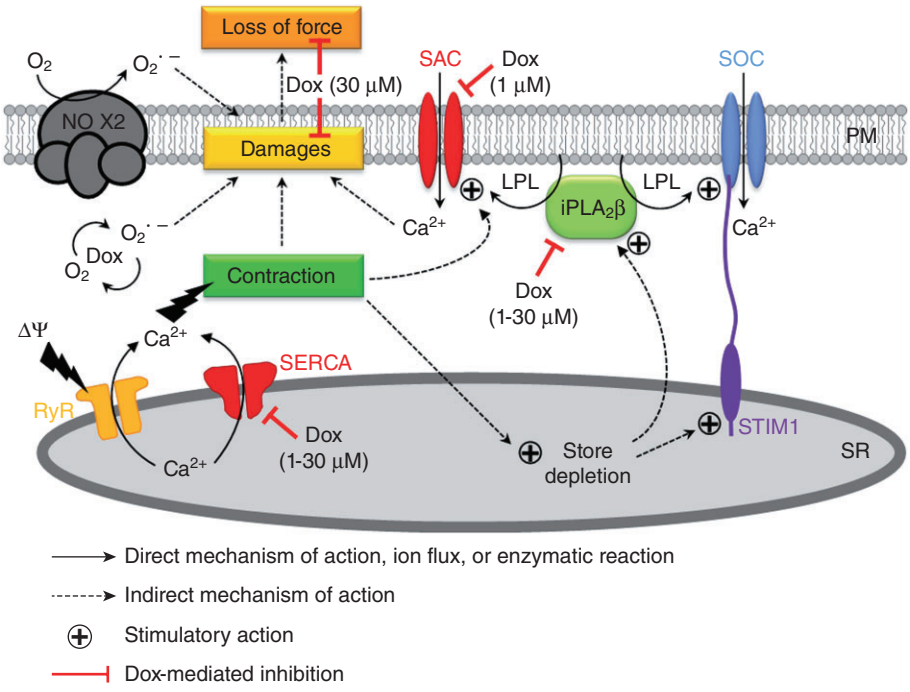

Figure 9

A possible model for the effects of Dox on iPLA$_2$β, SAC, SOC and fatigue in dystrophic muscle. In muscle cells, plasma membrane (PM) depolarization (ΔΨ) triggers opening of the ryanodine receptors (RyR) and release of Ca^{2+} from the sarcoplasmic reticulum (SR) into the cytosol, initiating muscle contraction that is terminated after Ca^{2+} re-uptake by the sarco/endoplasmic reticulum calcium ATPase (SERCA) pump. Sustained contractile activity causes Ca^{2+} depletion from the intracellular stores, which triggers Ca^{2+} entry directly via STIM1-mediated formation of store-operated channels (SOC) as well as indirectly via activation of iPLA$_2$β and release of lysophospholipids (LPLs). Contractile activity also stimulates Ca^{2+} entry through mechano-sensitive stretch-activated channels (SAC), which also respond to iPLA$_2$β-derived LPL. In dystrophic cells, the activity of SAC, SOC, iPLA$_2$β and NOX2 (a superoxide-generating enzyme) are reported to be enhanced, resulting in an excessive susceptibility to damages mediated by contraction, Ca^{2+} overload, oxidative stress and an increased muscle fatigability. The present report describes the effects of Dox on several targets involved in dystrophic pathogenesis (the concentrations of Dox required for significant effects are shown in parentheses). We found that Dox (1–30 μM)-inhibited iPLA$_2$β directly and, probably, indirectly (see text for details). Dox (1 μM) was also very efficacious for preventing SAC influx. In addition, we observed that Dox (1–30 μM) slightly inhibited SERCA activity and decreased mitochondrial Ca^{2+} uptake under condition that activates SAC (data not shown). As a result of these actions, and although Dox can produce superoxide through redox cycling, the net effect of Dox was to enhance recovery of muscle from eccentric contractions.

et al., 2006). The mechanisms by which iPLA$_2$β controls SOC are not fully clarified (Bolotina, 2008); however, we have shown earlier that in certain paradigms, its role may be prominent (Boittin *et al.*, 2006). Also, further data from our laboratory using various pharmacological compounds such as NOX inhibitors and lipoxygenase inhibitors confirm a good correlation between iPLA$_2$ inhibition and SOC blockade in muscle cell cultures (Ismail *et al.*, in preparation; Dorchies *et al.*, unpubl. data). On the other hand, other structurally unrelated compounds under testing in our laboratory, such as raloxifene and calmidazolium, failed to block SOC while reducing iPLA$_2$ activity, as reported here for Dox (Dorchies *et al.*, unpubl. data). The causes behind the apparent discrepancy between the fatty acid-releasing activity of iPLA$_2$, measured here by PED-6, and SOC inhibition might be the following: (i) the Dox-sensitive fatty acid-releasing activity of iPLA$_2$β might be independent of the ability of iPLA$_2$β to inhibit SOC; (ii) besides blocking iPLA$_2$β, Dox could have additional effects that compensate for iPLA$_2$-dependent SOC inhibition; and (iii) the crosstalk between the two pathways involved in SOC influx could compensate for the incomplete iPLA$_2$β inhibition seen in this work (Gwozdz *et al.*, 2012).

Besides the ability of Dox to inhibit iPLA$_2$β, our investigation reveals for the first time that Dox is a SAC inhibitor. This was evident at concentrations as low as 1 μM, and the effect was similar in extent to that produced by 300 μM streptomycin, a prototype SAC blocker, or by 30 μM GsMTx4, the most selective SAC blocker reported in the literature (Whitehead *et al.*, 2006).

Although the mechano-sensing process leading to SAC opening has not yet been clearly identified, TRP channels have received much attention (Holle and Engler, 2011). Lysophospholipids produced by PLA$_2$ have been shown to activate some members of this family, such as TRPV2 (Monet *et al.*, 2009) and TRPCs (Beech *et al.*, 2009). Hence, by inhibiting lysophospholipid formation by iPLA$_2$, Dox could inhibit activation of these channels.

The following cascade mechanism has also been suggested to activate SACs: Membrane stretch stimulates NOX, the resulting increase in ROS (as $O_2^{\bullet -}$) leads to activation of c-Src kinase, causing opening of SAC and Ca^{2+} influx (Allen *et al.*, 2010). Dox by binding to ferric ion in NOX (Gilliam and St Clair, 2011), or by modulating c-Src kinase activity could possibly inhibit this cascade. In a recent report,

Khairallah *et al*. (2012) showed that the microtubule network is responsible for the transmission of the mechano-transduction signal induced by muscle stretch to NOX. Disruptors of the microtubule network, such as colchicine, resulted in ROS inhibition and subsequently failure of SAC activation. Dox has also been reported to cause disruptions in the microtubules system in cardiomyocytes (Rabkin and Sunga, 1987). This could possibly be another explanation for the Dox-mediated SAC inhibitory effect observed here.

Mechanical stress, such as the one due to stretching contractions, causes Ca^{2+} influx into the muscle not only through SAC but also through membrane tears (McNeil and Khakee, 1992; Allen *et al*., 2010). Using an ionophore to increase intracellular Ca^{2+} levels, membrane damage occurred and protection was provided by PLA_2 inhibitors as well as by ROS scavengers (Duncan and Jackson, 1987; Howl and Publicover, 1990). Thus, the increased activity of $iPLA_2$, known to be present in dystrophic muscle (Lindahl *et al*., 1995; Boittin *et al*., 2006), would render the membrane more susceptible to mechanical damage, and hence increase Ca^{2+} influx through tears. Dox could counteract this effect by inhibition of $iPLA_2$.

To investigate the consequences of Dox action on SAC, and on the downstream local Ca^{2+} levels, targeted aequorin expression to the subsarcolemmal space was used. Dox also showed an inhibitory effect, which could not be attributed to $iPLA_2$ inhibition alone since *S*-BEL failed to do so. Indeed, our findings reveal that the concentration of Dox required for achieving full inhibition of $iPLA_2\beta$ (30 μM) is much higher than that required for blocking SAC activity (1 μM), which strongly suggest that Dox-mediated SAC inhibition is not primarily the consequence of $iPLA_2\beta$ inhibition.

To our knowledge, this is the first report demonstrating the ability of Dox to inhibit Ca^{2+} influx through SAC. We suggest that this effect is of clinical relevance to the cardiomyopathy induced by Dox in patients undergoing chemotherapy. SAC plays a role in heart adaptation to increased perfusion pressure. One of the heart's mechanisms to adapt to this is by increasing the force of contraction through activation of SAC (Calaghan and White, 2004). Dox, by inhibiting stretch-induced Ca^{2+} influx, would reduce this compensatory mechanism. This is consistent with an observation that was made in mice chronically treated with streptomycin: Treatment led to improved skeletal muscle function and quality, whereas the cardiac muscle deteriorated (Jorgensen *et al*., 2011).

Dox effects on isolated muscles

Isolated EDL and SOL muscles were used to assess functional effects. Dox neither affected force production nor contraction kinetics. High concentrations of Dox (up to 175 μM) were reported to reduce force and accelerate fatigue (Van Norren *et al*., 2009), but this was not observed at clinically relevant concentrations (1–5 μM) (Gilliam *et al*., 2009). Treatment of EDL muscles with Dox did not alter fatigability in the mild fatigue protocol.

S-BEL caused a rapid decline of force under repeated tetanic contractions. This is very likely due to an inhibition of SOC and impaired refilling of the Ca^{2+} stores, essential for maintaining force. Alternatively, this decline could be due to the ability of *S*-BEL to inhibit voltage-gated Ca^{2+} channels as has been shown in smooth muscle (Chakraborty *et al*., 2011), causing reduced excitation-contraction coupling and leading to force loss.

When the high-intensity protocol was used to induce fatigue, post-tetanic potentiation was observed in EDL, but not in the SOL, muscles. This was abolished in Dox and *S*-BEL-treated EDL muscles. Post-tetanic potentiation is commonly seen when muscles are exposed to repeated submaximal contractions, leading to an augmented force production before fatigue takes over. It is prevalent in fast twitch muscles, such as the EDL, almost absent in slow twitch muscles, such as the SOL (Hamada *et al*., 2000), due to phosphorylation of myosin light chains by the Ca^{2+}/calmodulin-dependent myosin light chain kinase (Zhi *et al*., 2005) and corresponds to our results. Our finding that Dox and *S*-BEL abolished this post-tetanic potentiation in EDL muscle strongly supports the idea that these compounds interfere with key mediators, such as Ca^{2+} signalling, phosphorylation status and ATP availability, leading to the disappearance of the initial potentiation phase and, ultimately, to acceleration of fatigue, which was also observed (Figure 7B). As mentioned above, other factors likely involved in these effects are Dox-mediated inhibition of SERCA (data not shown) and *S*-BEL-mediated inhibition of SOC; both of which would prevent proper refilling of the SR and eventually facilitate the loss of force as seen in EDL and SOL muscle.

Exposure of EDL muscles from mdx^{5Cv} mice to eccentric contractions resulted in greater force loss and reduced recuperation when compared with wild-type EDL muscles (Figure 8A). This has been attributed to an increased Ca^{2+} influx through either SAC or membrane tears, and subsequent activation of calpains causing protein degradation (Zhang *et al*., 2008; 2012). In the current study, Dox, which strongly blocked SAC, did not prevent the loss of force induced by eccentric contractions, but normalized post-injury recovery of the EDL muscle (Figure 8). In contrast, *S*-BEL, which inhibits both SAC and SOC activity, caused a dramatic loss of force that was further aggravated after cessation of the eccentric contractions (Figure 8). We propose that the impaired response of EDL muscles treated with *S*-BEL is due to SOC inhibition. This is not observed with Dox as it blocks SAC but not SOC.

What could be the links between Dox-mediated modulation of ROS, PLA_2 activity and muscle fragility?

Besides the role of $iPLA_2$ in modulating Ca^{2+} entry, it can also contribute to maintaining membrane homeostasis (Balboa and Balsinde, 2002). In fact, when ROS levels are elevated, membrane phospholipids become oxidized, and the resulting peroxides are preferentially cleaved by PLA_2 (Balboa and Balsinde, 2002). The $iPLA_2$ inhibitor *S*-BEL would disrupt this homeostatic mechanism, lead to a more vulnerable membrane and contribute to the diminished muscle resistance observed here. As both Dox and *S*-BEL inhibit $iPLA_2\beta$, one may suggest that a similar response to eccentric contractions should be seen after Dox or *S*-BEL treatment. However, our findings on recovery from eccentric contractions (Figure 8) show that this was not the case. The fact that Dox does not cause the same dramatic effects as *S*-BEL after eccentric contractions, although both compounds inhibit $iPLA_2\beta$ directly, may result from their differential ability (i) to accumulate

into biological membranes, generate ROS or promote the formation of lipid peroxides; (ii) to inhibit SOC and other targets; and (iii) to alter calcium handling and downstream calcium-dependent pathways through reduction of mitochondrial Ca^{2+} uptake and of SERCA pump activity (Ismail *et al.*, unpubl. data). Eventually, these differential properties of Dox and *S*-BEL would define specific sensitivities to stretch or tears upon damaging muscle contraction, resulting in toxicity with *S*-BEL but enhanced recovery with Dox.

Conclusion

Increased activity of $iPLA_2$ in muscle from DMD patients was reported over 15 years ago (Lindahl *et al.*, 1995); yet, to date, its role has not been fully clarified. In this study, we demonstrated the ability of Dox to inhibit $iPLA_2$ activity in cell cultures prepared from dystrophic and wild-type muscle and of the purified enzyme. For the first time, we report that Dox inhibits SAC. We also show that Dox was not detrimental to skeletal muscle function, but facilitated force recovery after damaging contractions.

Acknowledgements

This work was supported by grants from the Swiss National Science Foundation, the Association Française contre les myopathies (AFM, France) and the Duchenne Parent Project-The Netherlands (DPP-NL).

Conflicts of interest

None.

References

Ackermann EJ, Kempner ES, Dennis EA (1994). Calcium independent cytosolic phospholipase A_2 from macrophage-like $P338D_1$ cells – isolation and characterization. J Biol Chem 269: 9227–9233.

Alderton JM, Steinhardt RA (2000). Calcium influx through calcium leak channels is responsible for the elevated levels of calcium-dependent proteolysis in dystrophic myotubes. J Biol Chem 275: 9452–9460.

Allen DG, Gervasio OL, Yeung EW, Whitehead NP (2010). Calcium and the damage pathways in muscular dystrophy. Can J Physiol Pharmacol 88: 83–91.

Balboa MA, Balsinde J (2002). Involvement of calcium-independent phospholipase A_2 in hydrogen peroxide-induced accumulation of free fatty acids in human U937 cells. J Biol Chem 277: 40384–40389.

Balboa MA, Balsinde J, Jones SS, Dennis EA (1997). Identity between the Ca^{2+}-independent phospholipase A_2 enzymes from $P388D_1$ macrophages and Chinese hamster ovary cells. J Biol Chem 272: 8576–8580.

Bartoszek A (2002). Metabolic activation of adriamycin by NADPH-cytochrome P450 reductase; overview of its biological and biochemical effects. Acta Biochim Pol 49: 323–331.

Basset O, Boittin FX, Dorchies OM, Chatton JY, van Breemen C, Ruegg UT (2004). Involvement of inositol 1,4,5-trisphosphate in nicotinic calcium responses in dystrophic myotubes assessed by near-plasma membrane calcium measurement. J Biol Chem 279: 47092–47100.

Beech DJ, Bahnasi YM, Dedman AM, Al-Shawaf E (2009). TRPC channel lipid specificity and mechanisms of lipid regulation. Cell Calcium 45: 583–588.

Boittin FX, Petermann O, Hirn C, Mittaud P, Dorchies OM, Roulet E *et al.* (2006). Ca^{2+}-independent phospholipase A_2 enhances store-operated Ca^{2+} entry in dystrophic skeletal muscle fibers. J Cell Sci 119: 3733–3742.

Bolotina VM (2008). Orai, STIM1 and $iPLA_2$beta: a view from a different perspective. J Physiol 586: 3035–3042.

Brooks SV, Faulkner JA (1988). Contractile properties of skeletal-muscles from young, adult and aged mice. J Physiol 404: 71–82.

Burkholder TJ (2009). Stretch-induced ERK2 phosphorylation requires PLA_2 activity in skeletal myotubes. Biochem Biophys Res Commun 386: 60–64.

Cahalan MD (2009). STIMulating store-operated Ca^{2+} entry. Nat Cell Biol 11: 669–677.

Calaghan S, White E (2004). Activation of Na^+-H^+ exchange and stretch-activated channels underlies the slow inotropic response to stretch in myocytes and muscle from the rat heart. J Physiol 559: 205–214.

Chakraborty S, Berwick ZC, Bartlett PJ, Kumar S, Thomas AP, Sturek M *et al.* (2011). Bromoenol lactone inhibits voltage-gated Ca^{2+} and transient receptor potential canonical channels. J Pharmacol Exp Ther 339: 329–340.

Davies KJ, Doroshow JH (1986). Redox cycling of anthracyclines by cardiac mitochondria. I. Anthracycline radical formation by NADH dehydrogenase. J Biol Chem 261: 3060–3067.

Dorchies OM, Wagner S, Buetler TM, Ruegg UT (2009). Protection of dystrophic muscle cells with polyphenols from green tea correlates with improved glutathione balance and increased expression of 67LR, a receptor for (-)-epigallocatechin gallate. Biofactors 35: 279–294.

Ducret T, Vandebrouck C, Cao ML, Lebacq J, Gailly P (2006). Functional role of store-operated and stretch-activated channels in murine adult skeletal muscle fibres. J Physiol 575 (Pt 3): 913–924.

Duncan CJ, Jackson MJ (1987). Different mechanisms mediate structural changes and intracellular enzyme efflux following damage to skeletal-muscle. J Cell Sci 87: 183–188.

Fanchaouy M, Polakova E, Jung C, Ogrodnik J, Shirokova N, Niggli E (2009). Pathways of abnormal stress-induced Ca^{2+} influx into dystrophic mdx cardiomyocytes. Cell Calcium 46: 114–121.

Fu J, Yamamoto K, Guan ZW, Kimura S, Iyanagi T (2004). Human neuronal nitric oxide synthase one-electron reduction of adriamycin: role can catalyze of flavin domain. Arch Biochem Biophys 427: 180–187.

Gailly P (2002). New aspects of calcium signaling in skeletal muscle cells: implications in Duchenne muscular dystrophy. Biochim Biophys Acta 1600: 38–44.

Gaitanis A, Staal S (2010). Liposomal doxorubicin and nab-paclitaxel: nanoparticle cancer chemotherapy in current clinical use. Methods Mol Biol 624: 385–392.

Gilliam LAA, St Clair DK (2011). Chemotherapy-induced weakness and fatigue in skeletal muscle: the role of oxidative stress. Antioxid Redox Signal 15: 2543–2563.

Gilliam LAA, Ferreira LF, Bruton JD, Moylan JS, Westerblad H, Clair DKS *et al*. (2009). Doxorubicin acts through tumor necrosis factor receptor subtype 1 to cause dysfunction of murine skeletal muscle. J Appl Physiol 107: 1935–1942.

Gutierrez PL (2000). The metabolism of quinone-containing alkylating agents: free radical production and measurement. Front Biosci 5: D629–D638.

Gwozdz T, Dutko-Gwozdz J, Schafer C, Bolotina VM (2012). Overexpression of Orai1 and STIM1 proteins alters regulation of store-operated Ca^{2+} entry by endogenous mediators. J Biol Chem 287: 22865–22872.

Hamada T, Sale DG, MacDougall JD, Tarnopolsky MA (2000). Postactivation potentiation, fiber type, and twitch contraction time in human knee extensor muscles. J Appl Physiol 88: 2131–2137.

Hazen SL, Zupan LA, Weiss RH, Getman DP, Gross RW (1991). Suicide inhibition of canine myocardial cytosolic calcium-independent phospholipase A_2. Mechanism-based discrimination between calcium-dependent and -independent phospholipases A_2. J Biol Chem 266: 7227–7232.

Holle AW, Engler AJ (2011). More than a feeling: discovering, understanding, and influencing mechanosensing pathways. Curr Opin Biotechnol 22: 648–654.

Hopf FW, Turner PR, Steinhardt RA (2007). Calcium misregulation and the pathogenesis of muscular dystrophy. Subcell Biochem 45: 429–464.

Howl JD, Publicover SJ (1990). Permeabilzation of the sarcolemmal in mouse diaphragm exposed to BAY-K-8644 *in vitro*: time course, dependence on Ca^{2+} and effects of enzyme-inhibitors. Acta Neuropathol (Berl) 79: 438–443.

Hsu YH, Burke JE, Li S, Woods VL, Jr, Dennis EA (2009). Localizing the membrane binding region of group VIA Ca2+-independent phospholipase A2 using peptide amide hydrogen/deuterium exchange mass spectrometry. J Biol Chem 284: 23652–23661.

Jorgensen LH, Blain A, Greally E, Laval SH, Blamire AM, Davison BJ *et al*. (2011). Long-term blocking of calcium channels in mdx mice results in differential effects on heart and skeletal muscle. Am J Pathol 178: 273–283.

Jung K, Reszka R (2001). Mitochondria as subcellular targets for clinically useful anthracyclines. Adv Drug Deliv Rev 49: 87–105.

Khairallah RJ, Shi G, Sbrana F, Prosser BL, Borroto C, Mazaitis MJ *et al*. (2012). Microtubules underlie dysfunction in Duchenne muscular dystrophy. Sci Signal 5: ra56.

Lawler JM (2011). Exacerbation of pathology by oxidative stress in respiratory and locomotor muscles with Duchenne muscular dystrophy. J Physiol 589 (Pt 9): 2161–2170.

Lindahl M, Backman E, Henriksson KG, Gorospe JR, Hoffman EP (1995). Phospolipase A_2 activity in dystrophinopathies. Neuromuscul Disord 5: 193–199.

McHowat J, Swift LM, Arutunyan A, Sarvazyan N (2001). Clinical concentrations of doxorubicin inhibit activity of myocardial membrane-associated, calcium-independent phospholipase A_2. Cancer Res 61: 4024–4029.

McHowat J, Swift LM, Crown KN, Sarvazyan NA (2004). Changes in phospholipid content and myocardial calcium-independent phospholipase A_2 activity during chronic anthracycline administration. J Pharmacol Exp Ther 311: 736–741.

McNeil PL, Khakee R (1992). Disruptions of muscle fiber plasma membranes. Role in exercise-induced damage. Am J Pathol 140: 1097–1109.

Millay DP, Goonasekera SA, Sargent MA, Maillet M, Aronow BJ, Molkentin JD (2009). Calcium influx is sufficient to induce muscular dystrophy through a TRPC-dependent mechanism. Proc Natl Acad Sci U S A 106: 19023–19028.

Monet M, Gkika D, Lehen'kyi V, Pourtier A, Vanden Abeele F, Bidaux G *et al*. (2009). Lysophospholipids stimulate prostate cancer cell migration via TRPV2 channel activation. Biochim Biophys Acta 1793: 528–539.

Passaquin AC, Lhote P, Ruegg UT (1998). Calcium influx inhibition by steroids and analogs in C2C12 skeletal muscle cells. Br J Pharmacol 124: 1751–1759.

Petrof BJ, Shrager JB, Stedman HH, Kelly AM, Sweeney HL (1993). Dystrophin protects the sarcolemma from stresses developed during muscle contraction. Proc Natl Acad Sci U S A 90: 3710–3714.

Pinset C, Mulle C, Benoit P, Changeux JP, Chelly J, Gros F *et al*. (1991). Functional adult acetylcholine receptor develops independently of motor innervation in Sol 8 mouse muscle cell line. EMBO J 10: 2411–2418.

Rabkin SW, Sunga P (1987). The effect of doxorubicin (adriamycin) on cytoplasmic microtubule system in cardiac cells. J Mol Cell Cardiol 19: 1073–1083.

Reutenauer-Patte J, Boittin FX, Patthey-Vuadens O, Ruegg UT, Dorchies OM (2012). Urocortins improve dystrophic skeletal muscle structure and function through both PKA- and Epac-dependent pathways. Am J Pathol 180: 749–762.

Rizzuto R, Simpson AW, Brini M, Pozzan T (1992). Rapid changes of mitochondrial Ca^{2+} revealed by specifically targeted recombinant aequorin. Nature 358: 325–327.

Ruegg UT, Shapovalov G, Jacobson K, Reutenauer-Patte J, Ismail H, Dorchies OM *et al*. (2012). Store-operated channels and Ca2+ handling in muscular dystrophy. In: Groschner K, Graier WF, Romanin C (eds). Store-Operated Ca^{2+} Entry (SOCE) Pathways, 1st edn., Vol. 1. Springer: Wien, pp. 449–457.

Swift L, McHowat J, Sarvazyan N (2003). Inhibition of membrane-associated calcium-independent phospholipase A_2 as a potential culprit of anthracycline cardiotoxicity. Cancer Res 63: 5992–5998.

Swift L, McHowat J, Sarvazyan N (2007). Anthracycline-induced phospholipase A_2 inhibition. Cardiovasc Toxicol 7: 86–91.

Van Norren K, van Helvoort A, Argiles JM, van Tuijl S, Arts K, Gorselink M *et al*. (2009). Direct effects of doxorubicin on skeletal muscle contribute to fatigue. Br J Cancer 100: 311–314.

Wagner S, Dorchies OM, Stoeckel H, Warter JM, Poindron P, Takeda K (2003). Functional maturation of nicotinic acetylcholine receptors as an indicator of murine muscular differentiation in a new nerve-muscle co-culture system. Pflugers Arch 447: 14–22.

Whitehead NP, Streamer M, Lusambili LI, Sachs F, Allen DG (2006). Streptomycin reduces stretch-induced membrane permeability in muscles from mdx mice. Neuromuscul Disord 16: 845–854.

Wolf MB, Baynes JW (2006). The anti-cancer drug, doxorubicin, causes oxidant stress-induced endothelial dysfunction. Biochim Biophys Acta 1760: 267–271.

Zhang BT, Yeung SS, Allen DG, Qin L, Yeung EW (2008). Role of the calcium-calpain pathway in cytoskeletal damage after eccentric contractions. J Appl Physiol 105: 352–357.

Zhang BT, Whitehead NP, Gervasio OL, Reardon TF, Vale M, Fatkin D *et al*. (2012). Pathways of Ca^{2+} entry and cytoskeletal damage following eccentric contractions in mouse skeletal muscle. J Appl Physiol 112: 2077–2086.

Zhi G, Ryder JW, Huang J, Ding P, Chen Y, Zhao Y *et al*. (2005). Myosin light chain kinase and myosin phosphorylation effect frequency-dependent potentiation of skeletal muscle contraction. Proc Natl Acad Sci U S A 102: 17519–17524.

Zitt C, Strauss B, Schwarz EC, Spaeth N, Rast G, Hatzelmann A *et al*. (2004). Potent inhibition of Ca^{2+} release-activated Ca^{2+} channels and T-lymphocyte activation by the pyrazole derivative BTP2. J Biol Chem 279: 12427–12437.